NUCL SCI TECH (2016) 27:139
DOI 10.1007/s41365-016-0143-1

Analysis of the axial fitting clearance between the fuel rod and the end seat in CIADS

Ya-Feng Shu[1] · Yong-Wei Yang[1] · Xin Sheng[1] · Kang Chen[1] · De-Liang Fan[1] · Lu Zhang[1]

Received: 10 March 2016 / Revised: 20 June 2016 / Accepted: 22 June 2016 / Published online: 17 October 2016

Abstract The fuel assembly is key structure in China Initiative Accelerator Driven System, and the axial fitting clearance (AFC) for the fuel assembly design is an essential subject of study. In this paper, different methods are used to calculate critical stress in cylindrical shells. Because the thermal expansion of fuel assembly outer tube is larger than that of the cladding of fuel rod, enough space should be reserved between the upper end plug and upper seat slot. The collapse critical compressive stress of the cladding is obtained numerically through ANSYS simulation calculation. The AFC range between the fuel rod cladding and the end seat due to the displacement of thermal expansion is given by the theoretical formulas and ANSYS buckling analysis. These provide a reference for the AFC design of the reactor fuel assembly.

Keywords Thermal expansion · Critical stress · AFC calculation · ANSYS simulation

1 Introduction

Cylindrical shell, a common mechanical structure, has been widely used in aviation, aerospace, nuclear power, and other industries. In a nuclear reactor, fuel cladding and outer sleeve can be simplified as a cylindrical shell model, and axial fitting clearance (AFC) design of the fuel cladding and outer sleeve is important in China Initiative Accelerator Driven System [1]. Stability of cylindrical shells is also a hot spot of study [2–4]. Chen [5] and Zhao [6] did numerical buckling analysis of cylindrical shell under uniform axial compression in their thesis. Imani et al. [7] studied pellet cladding interaction (PCI).

As the fast reactor fuel rods are designed with high precision requirements for manufacturing and assembling [8], the thermal expansion of the fuel cladding and the end seat should be considered, and the structural thermal expansion gap is particularly important. Ishiwatari et al. [9] and Williamson et al. [10] studied the fuel behavior in different working conditions. Hofmeister et al. [11] laid a foundation for the fuel assembly design. In order to prevent the transition extrusion and the fuel rod buckling collapse from occurring, a certain compensation gap between the fuel rod end and its seat must be reserved.

In this paper, theoretical formulas to solve the cylindrical shell buckling problem are discussed for performing numerical simulations on the fuel cladding-end seat gap, toward engineering applications of the fuel rods in CIADS.

2 Model analysis

2.1 Problem description

In order to prevent buckling of the pellet cladding due to different thermal expansion of the materials, a certain gap (x_g) is reserved between a fuel rod and its outer sleeve assembly, as shown in Fig. 1.

This work was supported by the "Strategic Priority Research Program" of Chinese Academy of Sciences (No. XDA03030102).

✉ Yong-Wei Yang
yangyongwei@impcas.ac.cn

[1] Institute of Modern Physics, Chinese Academy of Sciences, Lanzhou 730000, China

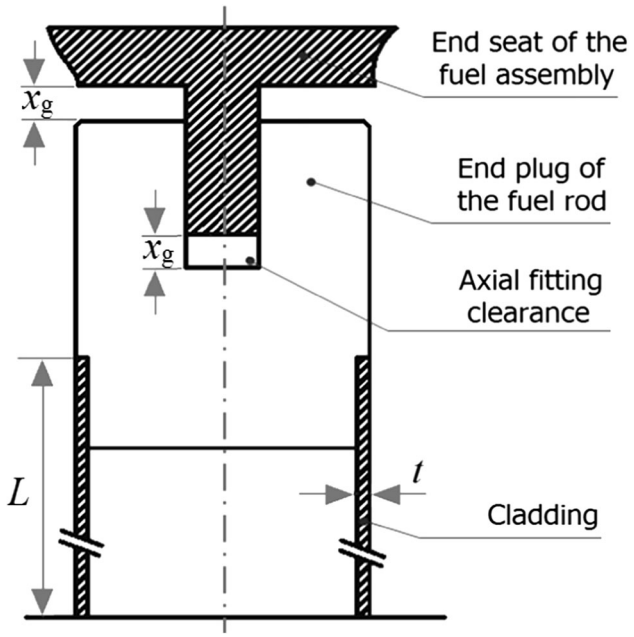

Fig. 1 Schematic view of end plug–end seat reserved space

2.2 Theoretical calculation of the critical stress

For cylindrical shell, a dimensionless shell length parameter $\chi = l^2/(Rt)$ is incorporated, where R is radius of the cylindrical shell middle surface, l is the cylindrical shell length, and t is the thickness. Axial cylindrical shells are classified into three categories [5], i.e., slender cylindrical shell ($\chi \leq 3.018$), middle length ($\chi > 3.018$), and short cylindrical shell ($\chi \geq 8.069\, R^2/t^2$). When the fuel rod axially fixed, it is subjected to axial force. For the three kinds of cylindrical shells with axial compression model, the critical stress can be calculated as follows.

For the slender cylindrical shell, the critical pressure load σ_{cr} can be obtained by the formula of Euler beam,

$$\sigma_{cr} = \pi^2 EI/\left[A(\mu l)^2\right], \tag{1}$$

where E is elastic or Young's modulus; $I = \pi(D^4 - d^4)/64$ is the cross-sectional moment of inertia, with d and D being the internal and external diameters of cylindrical shells, respectively; A is the cross-sectional area of cylindrical shell; and μ is length factor.

The critical load of the cylindrical shell can be calculated by Eq. (2) [12],

$$\sigma_{cr} = E(t/R)^3/\left[4\left(1-\upsilon^2\right)\right], \tag{2}$$

For middle or short length cylindrical shell, Eq. (3) can be applied based on the Donnell linear theory [3],

$$D'\mathrm{d}^4 w/\mathrm{d}x^4 + \sigma_x t + \mathrm{d}^2 w/\mathrm{d}x^2 + Etw/R^2 = 0, \tag{3}$$

where $D' = Et^3/[12(1-\upsilon^2)]$ is bending stiffness of cylindrical shell, with E being the elastic modulus and υ the Poisson' ratio; w is the lateral displacement, x is the axial coordinate, t is thickness of the cylindrical shell, R is the medium radius, and σ_x is the axial stress.

By solving Eq. (3), the critical stress σ_{cr} is obtained.

$$\sigma_{cr} = E(t/R)/\left[3\left(1-\upsilon^2\right)\right]^{1/2}. \tag{4}$$

However, the theoretical and experimental results are of great error [3]. Generally, an empirical formula is used to calculate the critical stress of a cylindrical shell of medium length:

$$\sigma_{cr} = 0.25Et/R. \tag{5}$$

3 Case study

A fuel rod referred to the design for China fast reactor [13] in the CIADS is shown schematically in Fig. 2. Its active region consists of fuel pellets stacked like "dish," top and bottom reflection layer, bob-weight, bottom end plug, gas chamber, gas gap, and cladding structure. For LMFBR, 316L is usually used as a candidate material for the cladding [14]. According to the ASME code, Section II, part D [15], the 316L physical parameters can be obtained in Table 1.

3.1 Temperature distribution of fuel cladding

The following formulas can be derived by the steady-state heat transfer equation [16],

$$q_L L = QC_{LBE}(T_o - T_i), R'\Delta T/\Phi = [\ln(T_o/T_i)]/(2\pi\lambda_c L), \tag{6}$$

where q_L is the fuel rod linear power density (W/mm) calculated by reactor physics analysis; $Q = \rho AV$ is mass flow (g/s), with ρ, A, and V being fluid density, the single flow channel area, and the flow velocity, respectively; C_{LBE} is the specific heat capacity (J g^{-1} °C) of coolant (lead bismuth eutectic) at constant pressure; λ_c is the thermal conductivity (W mm^{-1} $°C^{-1}$) of 316L; R' is the thermal resistance (°C/W); Φ is the heat flux (W); T_o is the outlet temperature (°C); and T_i is the inlet temperature (°C).

By Eq. (6), the temperature distribution of coolant can be calculated by:

$$T_o = q_L L/\left(QC_p\right) + T_i. \tag{7}$$

The heat balance equation is written as:

$$q_L L = \alpha\Omega \times \Delta T_\theta. \tag{8}$$

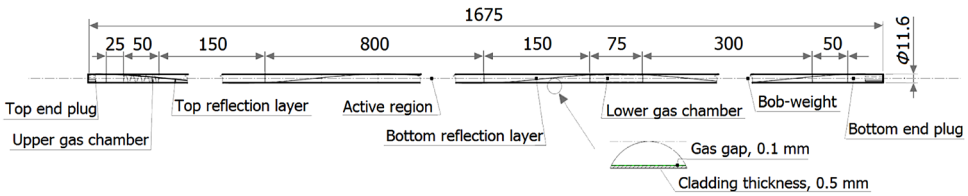

Fig. 2 Fuel rod structure (in mm)

Table 1 Physical parameters of 316L stainless steel

Temperature (°C)	250	275	300	325	350	375	400	425
Elastic modulus (GPa)	179	–	176	–	172	–	169	–
Coefficient of thermal expansion ($\times 10^{-6}$)	17.4	17.5	17.7	17.8	17.9	18.0	18.1	18.2
Thermal conductivity (W)	17.6	17.9	18.3	18.7	19.0	19.4	19.7	20.1

So, $\Delta T_\theta = q_L L/(\alpha\Omega)$, where ΔT_θ is the film temperature pressure of coolant and cladding, α is the convective heat transfer coefficient, and Ω is the heat transfer area (mm^2) of the heat exchange.

And thus, the temperature of outer surface of the shell is obtained by:

$$T_{os} = T + \Delta T_\theta, \tag{9}$$

where T is the temperature of coolant [17].

Through the discrete solution of Eq. (9), the temperature distribution of the cladding from Eq. (9) is shown in Fig. 3.

By Eq. (6), the temperature difference between inner and outer surface of fuel cladding can be derived as

$$\Delta T_c = R\prime\Phi = [q_L/(2\pi\lambda_c)]\ln(R_o/R_i). \tag{10}$$

From Eq. (10), the temperature difference is 2–3 °C. Thus, it can be neglected, and the average temperature of inner and outer surface of fuel cladding can be used as the cladding temperature. The temperature function of $T = 0.16x + 296.3$ is obtained by fitting the data in Fig. 3.

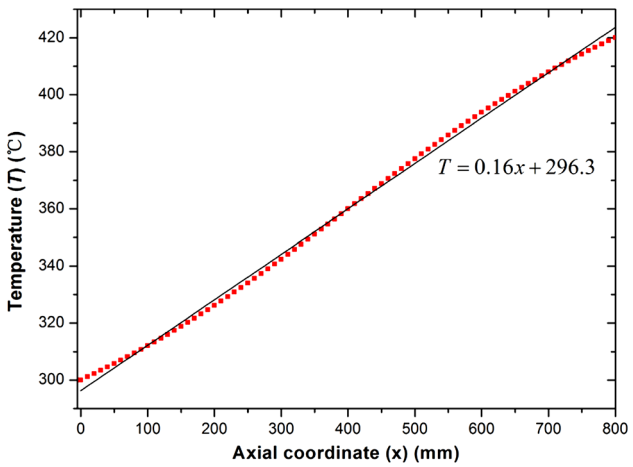

Fig. 3 Cladding temperature along the axis

3.2 Calculation of the gap for axial expansion of cladding

Radial deformation of the 0.5-mm-thick cladding is negligible, and the deformation of cladding is just axial deformation. If the shell deformation by thermal expansion is more than the reserve space of the upper end, the cladding can produce extrusion stress. The gap calculation is discussed as follows.

Thermal expansion coefficients of 316 L at different temperatures in Table 1 can be fitted by $K(T) = 4 \times 10^{-9}T + 16.5 \times 10^{-6}$.

In this paper, the thermal expansion is obtained from ASME code, section II [15]. The calculation length of the cladding and the outer sleeve is $L = 1675$ mm. For Δx, the thermal expansion can be written as $\Delta\delta = K(T)\ \Delta x\Delta T$, where $\Delta T = T - 25$ is the temperature changes by setting reference temperature at 25 °C.

For the active region, the total deformation is.

$$\delta_{active} = \int_0^L (K \times \Delta T)\mathrm{d}x. \tag{11}$$

On substituting the parameters into Eq. (11), we have $\delta_{active} = 4.562$ mm.

In addition to active region of the fuel rod, the lengths of upper and lower non-active region of the cladding are calculated to be $L_{lower} = L_{upper} = 575$ mm. In the active region, the cladding temperature change is so small that the expansion can be calculated based on the average temperatures,

$$\begin{aligned} \Delta L_{lower} &= K_{300}L_{lower}(300 - 25) = 2.081\,\text{mm}, \\ \Delta L_{upper} &= K_{421}L_{upper}(421 - 25) = 1.982\,\text{mm}, \\ \Delta L_{total} &= \delta_{active} + \Delta L_{lower} + \Delta L_{upper} = 8.625\,\text{mm}, \end{aligned} \tag{12}$$

where K_{300} and K_{421} is the thermal expansion coefficient of the lower and upper parts.

By applying a fixed constraint to the lower end of cladding and the temperature function in Fig. 3, the

displacement of cladding in the active region can be calculated by the ANSYS code (Fig. 4).

Comparing simulation results in Fig. 5 with the calculation results, we can see that the radial thermal deformation has a greater influence than the axial thermal deformation, and thus

$$\Delta L_{\text{total}} = 6.40 + \Delta L_{\text{lower}} + \Delta L_{\text{upper}} = 10.46 \text{ mm}$$

From thermal hydraulic calculation, the outer sleeve temperature distributes linearly, and temperature changes in the outer sleeve can be obtained by Eq. (13),

$$T' = 0.072x + 250. \quad (13)$$

Taking Eq. (13) into Eq. (11), the thermal deformation is 5.107 mm.

Thermal deformations of the outer sleeve calculated by the ANSYS code are shown in Fig. 5. Through linear buckling analysis using the ANSYS code, critical stresses of the cladding under axial compression are shown in Fig. 6.

3.3 Analysis and discussion of the result

Because of the calculation results of ANSYS taking into account the influence of the radial to the axial direction, the total deformation of the cladding is 2.09 mm larger than that of the outer sleeve.

Buckling critical stresses calculated using Eq. (1) and APDL ANSYS code are 9.33 and 1.04 MPa, respectively; while the critical stress of cladding collapse calculated using Eq. (2) is 37.7 MPa.

The three calculation methods above can obtain critical stress of cladding failure, with the empirical formula of Eq. (2) giving the largest result. In the reactor, the fuel rod load in addition to the axial pressure include the coolant and chamber gas, so the balance of radial load increases the

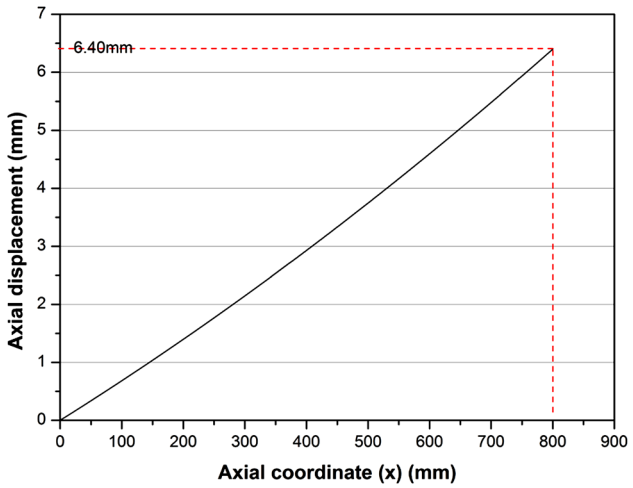

Fig. 4 ANSYS-simulated displacement of cladding in axial direction

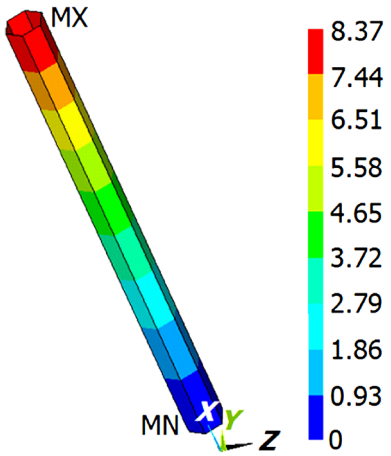

Fig. 5 Displacement contour of the outer sleeve at axial direction

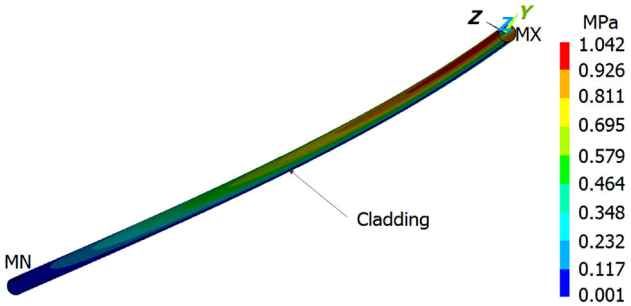

Fig. 6 Critical stress of the linear buckling for cladding

structure stability. Therefore, the gap is calculated using Eq. (2).

According to the critical stress, the average strain can be estimated at

$$\varepsilon = \sigma_{\text{cr}}/E = 1.38 \times 10^{-4}. \quad (14)$$

Then, the allowed compress value of the fuel rods is $\Delta L = \varepsilon L = 0.23$ mm. Therefore, to prevent the fuel rod buckling, the gap range is 1.86–2.09 mm.

4 Conclusion

In this paper, three kinds of critical stress calculation methods about cylindrical shells under different shell length are analyzed and obtained. The temperature distribution of cladding is calculated which is based on nuclear reactor physics and heat transfer calculation for CIADS fuel rod. The temperature difference between inlet and outlet is about 120 °C. Finally, the thermal expansion gap reserved is obtained, which is vital of importance for the design of fuel rod assembly. Besides, the calculation method of thermal expansion gap is studied; the results of three calculation methods are compared and analyzed.

Through the analysis, it is found that the optimal method to calculating the reserved clearance is the second method using Eq. (2). The gap between the end plug and the end seat is 1.86–2.09 mm.

References

1. W.L. Zhan, H.S. Xu, Advanced fission energy program—ADS transmutation system. Bull. Chin. Acad. Sci. **27**, 375–383 (2012). doi:10.3969/j.issn.1000-3045.2012.03.017
2. M.S. Ismail, J. Purbolaksono, A. Andriyana et al., The use of initial imperfection approach in design process and buckling failure evaluation of axially compressed composite cylindrical shells. Eng. Fail. Anal. **51**, 20–28 (2015). doi:10.1016/j.engfailanal.2015.02.017
3. L.Y. Chu, Experiment and numerical analysis of axial elastic and plastic buckling of welded cylindrical shells. Ph. D. Thesis, Zhe Jiang University (2012)
4. H. Qian, The analysis on elastic and plastic stability of cylindrical shell. Master Thesis, Wuhan University of Technology (2002)
5. X.G. Chen, Numerical buckling analysis and optimization of cylindrical shell under uniform axial compression. Ph. D. Thesis, Beijing University of Technology (2009)
6. Z. Yang, G.T. Jin, Stability design of axially compressed the cylindrical shells. Eng. Mech. **20**, 116–126 (2003). doi:10.3969/j.issn.1000-4750.2003.06.021
7. M. Imani, M. Aghaie, A. Zolfaghari et al., Numerical study of fuel–clad mechanical interaction during long-term burnup of WWER1000. Ann. Nucl. Energy **80**, 267–278 (2015). doi:10.1016/j.anucene.2015.01.036
8. A. Alemberti, J. Carlsson, E. Malambu et al., European lead fast reactor—ELSY. Nucl. Eng. Des. **241**, 3470–3480 (2011). doi:10.1016/j.nucengdes.2011.03.029
9. H. Ju, Y. Ishiwatari, Y. Oka, Fuel rod behavior under normal operating conditions in Super Fast Reactor with high power density. Nucl. Eng. Des. **289**, 166–174 (2015). doi:10.1016/j.nucengdes.2015.04.037
10. R.L. Williamson, J.D. Hales, S.R. Novascone et al., Multidimensional multiphysics simulation of nuclear fuel behavior. J. Nucl. Mater. **423**, 149–163 (2012). doi:10.1016/j.jnucmat.2012.01.012
11. J. Hofmeister, C. Waata, J. Starflinger et al., Fuel assembly design study for a reactor with supercritical water. Nucl. Eng. Des. **237**, 1513–1521 (2007). doi:10.1016/j.nucengdes.2007.01.008
12. China Guangzhou Nuclear Power Engineering Co., Ltd. PWR nuclear island design 4th vol (Atomic Energy Press, Beijing, China, 2010), pp. 55–56
13. G.S. Xie, R.X. Zhang, *Fast Neutron Reactor Fuel Element* (Chemical Industry Press, Beijing, 2007), pp. 54–129
14. H.A. Abderrahim, V. Sobolev, E. Malambu, et al., Fuel design for the experimental ADS MYRRHA. Technical Meeting on use of LEU in ADS. IAEA, (Viena, Austria, 2005), pp. 1–13
15. ASME Boiler and Pressure Vessel Code, Section II: Materials, Part D: Properties. (American Society of Mechanical Engineers, New York, USA, 2010), pp. 707–744
16. S.M. Yang, W.Q. Tao, *Heat Transfer* (High Education Press, Beijing, 2007), pp. 34–53
17. W.L. Huang, R.Y. Sa, D.N. Zhou et al., Experimental study on fragmentation behaviors of molten LBE and water contact interface. Nucl. Sci. Tech. **26**, 060601 (2015). doi:10.13538/j.1001-8042/nst.26.060601